

Probing the time variation of fine structure constant using galaxy clusters and quintessence model

ZHI-E LIU(刘志娥) ¹, WEN-FEI LIU(刘文斐),¹ TONG-JIE ZHANG(张同杰) ^{1,2}, ZHONG-XU ZHAI(翟忠旭),³ AND
KAMAL BORA ⁴

¹*College of Physics and Electronic Engineering, Qilu Normal University
Jinan 250200, China*

²*Department of Astronomy, Beijing Normal University
Beijing 100875, China*

³*IPAC, California Institute of Technology
Mail Code 314-6, 1200 E. California Blvd., Pasadena, CA 91125*

⁴*Department of Physics, Indian Institute of Technology
Hyderabad, Kandi, Telangana-502284, India*

Submitted to ApJ

ABSTRACT

We explore a possible time variation of the fine structure constant ($\alpha \equiv e^2/\hbar c$) using the Sunyaev-Zel'dovich effect measurements of galaxy clusters along with their X-ray observations. Specifically, the ratio of the integrated Compton-ionization parameter $Y_{SZ}D_A^2$ and its X-ray counterpart Y_X is used as an observable to constrain the bounds on the variation of α . Considering the violation of cosmic distance duality relation, this ratio depends on the fine structure constant as $\sim \alpha^3$. We use the quintessence model to provide the origin of α time variation. In order to give a robust test on α variation, two galaxy cluster samples, the 61 clusters provided by the Planck collaboration and the 58 clusters detected by the South Pole Telescope, are collected for analysis. Their X-ray observations are given by the XMM-Newton survey. Our results give $\zeta = -0.203_{-0.099}^{+0.101}$ for the Planck sample and $\zeta = -0.043_{-0.148}^{+0.165}$ for the SPT sample, indicating that α is constant with redshift within 3σ and 1σ for the two samples, respectively.

Keywords: Quintessence (1323) — Cosmological models (337) — Galaxy clusters (584)

1. INTRODUCTION

The fine structure constant $\alpha \equiv e^2/\hbar c$ is at the central position in the system of fundamental physical constants. It measures the strength of the electromagnetic interaction between charged elementary particles in the low-energy limit. Recently, the fine structure constant was determined at an unprecedented precise, that is, $\alpha^{-1} = 137.035999206$ with a relative accuracy of 81 parts per trillion (Morel et al. 2020). However, in 1937, Dirac argued that the fundamental constants of Nature may not be pure constants but vary slowly with the epoch, and he proposed a gravitational ‘constant’ decreasing proportionally to t^{-1} (Dirac 1937). Since then, some theoretical and experimental investigations allowing space-time variation of fundamental constants have been put into effect (Martins 2017; Uzan 2011, 2003; Wang & Chen 2020). In order to remedy the dire consequence (Teller 1948) induced by the varying gravitational constant $G \sim t^{-1}$, Gamow (in 1967) suggested that e^2 increases in direct proportion to the age of the universe (Gamow 1967). Phenomenological models that usually assumed an α varying as some power-law or logarithm of time, like those introduced by Gamow, represent the early work of studying varying α (Barrow & Tipler 1986).

Over the last few decades, the focus has shifted to various extensions of standard models, in which one or more fundamental constants of Nature become dynamical quantities. The first self-consistent theory of varying α is the framework constructed by [Bekenstein \(1982\)](#) via modifying Maxwell electrodynamics, which was then extended to a cosmological setting by [Sandvik et al. \(2002\)](#); [Barrow et al. \(2002b\)](#); [Barrow & Mota \(2003\)](#); [Barrow et al. \(2002a\)](#), namely BSBM theory. In the BSBM model, variations in α occur due to a coupling between the electromagnetic field and a massless scalar field in the action. The original BSBM model was then extended by adding a non-trivial potential ([Barrow & Li 2008](#); [Farajollahi & Salehi 2012](#)), or by allowing the coupling between scalar field ϕ and photons as a function of ϕ ([Barrow & Lip 2012](#)), or by allowing for both an arbitrary coupling and potential function ([Barrow & Graham 2013](#)). Another class of extensions of standard models are based on the belief that space has more than three dimensions, and the extra space dimensions can cause varying fundamental constants ([Chodos & Detweiler 1980](#); [Marciano 1984](#); [Kolb et al. 1986](#); [Barrow 1987](#)). For instance, in Kaluza-Klein theories, the time evolution of the mean KK radius R_{KK} of extra spatial dimensions can give rise to time variations of fundamental constants ([Marciano 1984](#)).

At present, observational data of α variation are becoming increasingly abundant. The cosmic microwave background (CMB) data ([O’Bryan et al. 2015](#); [PLANCK Collaboration 2015](#); [Hart & Chluba 2018](#)) and the Big Bang nucleosynthesis (BBN) ([Iocco et al. 2009](#); [Mosquera & Civitaresse 2013](#); [Clara & Martins 2020](#)) can constrain α variations in the early universe. The Planck Collaboration obtained $\Delta\alpha/\alpha \approx 10^{-3}$ at redshift $z \approx 10^3$ by analyzing the CMB spectra ([PLANCK Collaboration 2015](#)), and the constraints given by the abundance of the light elements emerged during BBN are not very tight (approximately $\Delta\alpha/\alpha < 10^{-2} - 10^{-3}$ at $z \approx 10^9 - 10^{10}$), too ([Mosquera & Civitaresse 2013](#)). The 1.8 billion-year-old natural nuclear reactor at the Oklo Uranium Mine in Gabon can give much tighter bounds on the time variations of α ($\Delta\alpha/\alpha \approx 10^{-7} - 10^{-8}$) ([Damour & Dyson 1996](#); [Lamoreaux & Torgereson 2004](#)). The most sensitive constraints on $\Delta\alpha/\alpha$ were achieved at $z \approx 1 - 6$ from the spectral lines significantly affected by relativistic effects in absorbing clouds around distant quasars. The quasar absorption lines observed by Keck/HIRES and VLT/UVES telescopes have produced a large data sample that describe the dependence of $\Delta\alpha/\alpha$ on redshift z , in which the variations of α are normally constrained by $\Delta\alpha/\alpha \approx 10^{-5} - 10^{-6}$ ([Murphy et al. 2001b,c,a, 2003, 2004, 2007, 2008](#); [Chand et al. 2004](#); [Srianand et al. 2004](#); [Webb et al. 1999, 2001](#)). In addition, the spatial variations of α observed by comparing the results from Keck and VLT have also got interest of study. Specifically, at $z > 1.8$ the Northern sky observations of the Keck telescope suggested a smaller value of the fine structure constant ($\Delta\alpha/\alpha = (-0.74 \pm 0.17) \times 10^{-5}$), but the Southern sky observations of the VLT telescope showed an increasing fine structure constant ($\Delta\alpha/\alpha = (0.61 \pm 0.20) \times 10^{-5}$) ([Webb et al. 2011](#); [King et al. 2012](#)). This could be due to an undetected systematic effects, but may also hint to a new physics. More recently, a constraint on the relative variation of α below 10^{-5} is obtained by comparing the absorption lines of late-type evolved giant stars from the S star cluster orbiting the supermassive black hole in our Galactic Center with the absorption lines in the lab ([Hees et al. 2020](#)). The absorption lines of white dwarf stars can also be used to constrain $\Delta\alpha/\alpha$ ([Berengut et al. 2013](#)).

Some work considers a class of dilaton runaway models, where $\Delta\alpha/\alpha = -\gamma \ln(1+z)$, and indirectly constrains $\Delta\alpha/\alpha$ by constraining γ . Most of this kind of work employed the observations of the Sunyaev-Zeldovich effect combined with observations of the X-ray surface brightness of galaxy clusters, for which the former can be characterized by the integrated Compton-ionization parameter $Y_{SZ}D_A^2$ and the latter by the Y_X parameter ([Holanda et al. 2017](#); [Bora & Desai 2021a](#); [Colaço et al. 2019](#); [Holanda et al. 2016a,b](#); [Bora & Desai 2021b](#)). Alternatively, Colaço et al. used combined measurements of Strong Gravitational Lensing systems and Type Ia Supernovae to constrain γ ([Colaço et al. 2020b,a](#)). Instead of based on runaway models, Galli assumed that α can linearly vary with redshift, i.e., $\alpha/\alpha_0 = A_{lin}(1+z)$, and then studied whether α is time-dependent by constraining A_{lin} using the Sunyaev-Zeldovich effect and its X-ray counterpart of galaxy clusters ([Galli 2013](#)).

In this paper, we will consider a specific model for the variation of the fine structure constant α driven by a typical quintessence scenario, i.e. a linear coupling with the electromagnetic term in the Lagrangian.

2. COUPLING OF QUINTESSENCE TO THE ELECTROMAGNETIC FIELD

Quintessence is one type of dynamical scalar field models ([Padmanabhan 2003](#)). It has been used to model the dark energy component in the universe. We expect the quintessence field to couple with the electromagnetic sector of the matter-radiation Lagrangian and induce a time variation of the fine structure constant α . The general form of the action involving a quintessence scalar field and its coupling with the electromagnetic term can be written as ([Marra](#)

& Rosati 2005)

$$S = \frac{1}{16\pi G} \int d^4x \sqrt{-g} R + \int d^4x \sqrt{-g} \left[\frac{1}{2} \partial^\mu \phi \partial_\mu \phi - V(\phi) \right] - \frac{1}{4} \int d^4x \sqrt{-g} B_F(\phi) F_{\mu\nu} F^{\mu\nu} + \int d^4x \sqrt{-g} \mathcal{L} \quad (1)$$

where G is the Newton's Gravitational constant and \mathcal{L} represents the Lagrangian density including the Standard Model fields and a hypothetical dark matter sector. $B_F(\phi)$ describes the coupling between quintessence and the electromagnetic field and allows for the evolution in ϕ . The effective fine structure constant depends on the value of ϕ as (Copeland et al. 2004)

$$\alpha(\phi) = \frac{\alpha_0}{B_F(\phi)}. \quad (2)$$

where α_0 is the fine structure constant measured today. Therefore, we get the relative variation of α :

$$\frac{\Delta\alpha}{\alpha} \equiv \frac{\alpha(t) - \alpha_0}{\alpha_0} = \frac{1 - B_F(\phi)}{B_F(\phi)}. \quad (3)$$

We consider a homogeneous and isotropic FRW cosmology described by the line element

$$ds^2 = -dt^2 + a^2(t) \left[\frac{dr^2}{1 - Kr^2} + r^2(d\theta^2 + \sin^2\theta d\varphi^2) \right] \quad (4)$$

where $a(t)$ and K are the scale factor and spatial curvature respectively. Combining Eq.(1) and Eq.(4) can yield equations describing the evolution of the quintessence scalar field in the FRW universe, that is, the Friedmann equation (Park & Ratra 2019)

$$\left(\frac{H}{H_0} \right)^2 = \frac{1}{1 - \frac{1}{6}(\phi')^2} \left[\Omega_m a^{-3} + \Omega_r a^{-4} + \Omega_k a^{-2} + \frac{V(\phi)}{3H_0^2} \right] \quad (5)$$

and the Klein-Gordon equation (Park & Ratra 2019)

$$\phi'' + \left(3 + \frac{\dot{H}}{H^2} \right) \phi' + \frac{dV(\phi)}{d\phi} \frac{1}{H^2} = 0, \quad (6)$$

where $\phi' \equiv d\phi/d \ln a$, and an overdot denotes the time derivative d/dt . We have set the present scale factor $a_0 = 1$ and chosen the units such that the Newtonian gravitational constant $G \equiv 1/8\pi$. $H = \dot{a}/a$ is the Hubble parameter and H_0 is the Hubble constant. The present value of the non-relativistic matter density parameter Ω_m is the sum of present baryonic matter and CDM density parameters, $\Omega_m = \Omega_b + \Omega_c$, Ω_r is the present value of the radiation density parameter, and Ω_k is the present value of the spatial curvature density parameter. We assume a spatially flat universe, $\Omega_k = 0$, and set $\Omega_m = 0.315 \pm 0.007$, $H_0 = 67.4 \pm 0.5 \text{ km s}^{-1} \text{ Mpc}^{-1}$ according to the Planck 2018 results (Planck Collaboration 2020; Chen et al. 2019). Ω_r is not a free parameter but determined by $\Omega_r = \Omega_m a_{eq}$, where a_{eq} is the scale factor at the epoch of matter-radiation equality given by $a_{eq} = \frac{4.15 \times 10^{-5}}{\Omega_m h^2}$ (Dodelson & Schmidt 2020). Here $h = H_0/(100 \text{ km s}^{-1} \text{ Mpc}^{-1})$.

A general functional form of the quintessence potential $V(\phi)$ can be written as a combination of power-law and exponential functions. Copeland et al. (2004) discussed in detail the effect induced by different quintessence models on the cosmological $\Delta\alpha$. In our work, we only consider an inverse power-law potential (Peebles & Ratra 1988; Samushia & Ratra 2006, 2009; Chen & Ratra 2011; Park & Ratra 2019)

$$V(\phi) = V_1 \phi^{-n} \quad (7)$$

where V_1 and n are non-negative constant parameters. In the limit $n = 0$ the quintessence dark energy becomes the cosmological constant Λ . The exponent parameter n has been constrained to $[0, 6]$ by various observational data (Park & Ratra 2019). Marra & Rosati (2005) showed that choosing different quintessence potentials gives a subdominant effect on the cosmological variation of α with respect to changing the coupling function $B_F(\phi)$. Our tests also show that different values of n only have a mild impact on the result, and fixing this parameter can improve the efficiency

of the computation significantly. Thus, following [Marra & Rosati \(2005\)](#) we set $n = 1.0$ in order to have the correct attractor equation of state ([Marra & Rosati 2005](#)). By definition, the pressure p_ϕ and energy density ρ_ϕ of the scalar field are given by

$$\begin{aligned} p_\phi &= \frac{\dot{\phi}^2}{2} - V(\phi), \\ \rho_\phi &= \frac{\dot{\phi}^2}{2} + V(\phi), \end{aligned} \quad (8)$$

and the equation of state for scalar field is $\omega_\phi = p_\phi/\rho_\phi$. The coefficient parameter V_1 of the potential (7) can be numerically calculated by making the energy density today $\rho_\phi^{(0)}$, which is evolved from equation (6), equal to

$$\rho_{cr}\Omega_\phi = \rho_{cr}(1 - \Omega_m - \Omega_r - \Omega_k), \quad (9)$$

where $\rho_{cr} = 3H_0^2$ is the critical density. Thus, V_1 is in fact determined by n implicitly. Accordingly, the dark energy density parameter today is $\Omega_\phi = \rho_\phi^{(0)}/\rho_{cr} = (\phi_0')^2/6 + V(\phi_0)/(3H_0^2)$, where ϕ_0 and ϕ_0' are the current values of ϕ and ϕ' .

We numerically solve the cosmological equations (5)-(6) and then produce the resulting $\Delta\alpha$ at a series of redshifts. We use the initial conditions ([Peebles & Ratra 1988](#))

$$\phi = \left[\frac{2}{3}n(n+2) \right]^{1/2} \left(\frac{a}{a_1} \right)^{3/(n+2)} \quad (10)$$

at scale factor $a_i = 10^{-10}$. Here a_1 denotes the characteristic epoch at which the dominant mass density switches from ordinary matter to the ϕ field.

Equation (3) shows the evolution of α depends on the evolution of ϕ via a concrete functional form of $B_F(\phi)$, so what follows is the choice of $B_F(\phi)$. In principle, there are no constraints on the form of $B_F(\phi)$. [Marra & Rosati \(2005\)](#) proposed a general form of the function $B_F(\phi)$ which is characterized by a set of four parameters, and comprehensively discussed various $B_F(\phi)$ cases that gave different α histories. In this work we adopt the simplest case that is originally proposed by [Bekenstein \(1982\)](#), i.e. a linear dependence on ϕ such that

$$B_F(\phi) = 1 - \zeta(\phi - \phi_0) \quad (11)$$

where ϕ_0 denotes the present quintessence, and ζ is a parameter describing the strength of the coupling between quintessence and the electromagnetic field and to be determined by the observational data. The case $\zeta = 0$, or $B_F(\phi) = 1$, means there is no coupling to the electromagnetic field, and thus the fine structure constant α really stays a constant during the lifetime of the universe. Substituting Eq.(11) into Eq.(3) results in

$$\frac{\Delta\alpha}{\alpha} = \zeta(\phi - \phi_0). \quad (12)$$

3. $Y_{SZ} - Y_X$ RELATION AND α

The Sunyaev-Zel'dovich Effect (Y_{SZ}) and X-ray surface brightness (Y_X) are two observable quantities of galaxy clusters. Since Y_{SZ} and Y_X both reflects the thermal energy of the cluster and are proportional to the total cluster mass, their ratio $Y_{SZ}D_A^2/Y_X$ should be a constant independent of redshift. This ratio has been used to explore the variation of α ([Galli 2013](#); [Colaço et al. 2019](#); [Holanda et al. 2016b](#); [Bora & Desai 2021a,b](#)), which is also our main focus in this paper.

The high energy electrons in the ionized intergalactic gas of galaxy clusters can scatter the CMB photons, via Inverse Compton Effect, resulting in the distortion of the CMB spectrum. This is the known Sunyaev-Zel'dovich effect (SZ, hereafter) ([Sunyaev & Zel'dovich 1972](#)). The CMB spectral distortion caused by SZ effect is proportional to the Compton parameter y , which is expressed as

$$y = \frac{\sigma_T k_B}{m_e c^2} \int n_e T dl = \frac{\sigma_T}{m_e c^2} \int P dl \quad (13)$$

where k_B is the Boltzmann constant, c is the speed of light, m_e is the electron mass, n_e is the number density of electrons, T is the electron temperature, and $P = n_e k_B T$ is the pressure of the intracluster medium under the

assumption of ideal gas equation of state. Therefore, the Compton parameter quantifies the gas pressure of the intracluster medium integrated along the line of sight. The Thompson cross-section σ_T can be computed using Feynman diagrams and linked to the fine structure constant α by

$$\sigma_T = \frac{8\pi}{3} \left(\frac{e^2}{m_e c^2} \right)^2 = \frac{8\pi}{3} \left(\frac{\hbar^2 \alpha^2}{m_e^2 c^2} \right) \quad (14)$$

Integrating the Compton parameter y over the plane perpendicular to the line of sight can provide the spherical integrated Compton parameter, defined as

$$Y_{SZ} D_A^2 = \int y dA = \frac{\sigma_T k_B}{m_e c^2} \int n_e T dV = \frac{\sigma_T}{m_e c^2} \int P dV. \quad (15)$$

Thus, we can see that $Y_{SZ} D_A^2$ depends on the fine structure constant through the Thompson cross-section (see Eq.(14)) as (Galli 2013)

$$Y_{SZ} D_A^2 \propto \alpha^2. \quad (16)$$

According to Eq.(2), we have

$$Y_{SZ} D_A^2 \propto B_F^{-2}(\phi). \quad (17)$$

The intergalactic hot gas emits mainly through thermal bremsstrahlung. The magnitude of the X-ray emission is quantified by the Y_X parameter which can be acquired by X-ray surface brightness observations and is defined as (Kravtsov et al. 2006)

$$Y_X = M_g(R) T_X, \quad (18)$$

where $M_g(R)$ is the X-ray determined gas mass within the radius R and T_X is the X-ray temperature of the cluster. It has been shown that $M_g(R)$ can be written as (Goncalves et al. 2012; Colaço et al. 2019)

$$M_g(< \theta) \propto \alpha^{-3/2} D_L D_A^{3/2} \quad (19)$$

where D_L is the luminosity distance. This equation shows $M_g(R)$ depends not only on the fine structure constant but also on the validity of the cosmic distance duality relation (CDDR), $D_L = (1+z)^2 D_A$. A variation of α will lead to a violation of the CDDR (Hees et al. 2014), which is normally described as $D_L = \eta(z)(1+z)^2 D_A$. Consequently, Y_X will scale to $\alpha(z)$ and $\eta(z)$ by

$$Y_X \propto M_g(< \theta) \propto \alpha(z)^{-3/2} \eta(z) \quad (20)$$

According to the scalar field theory, $\alpha(z)$ and $\eta(z)$ are linked by (Hees et al. 2014)

$$\frac{\Delta\alpha}{\alpha} \equiv \frac{\alpha(z) - \alpha_0}{\alpha_0} = \eta(z)^2 - 1. \quad (21)$$

Together with Eq.(2) we have

$$Y_X \propto \alpha^{-1} \propto B_F(\phi). \quad (22)$$

Then, based on Eqs.(17) and (22), the dimensionless ratio of $Y_{SZ} D_A^2$ to Y_X can be related to the coupling strength $B_F(\phi)$ by

$$\frac{Y_{SZ} D_A^2}{Y_X} \propto B_F(\phi)^{-3}. \quad (23)$$

This ratio can also be expressed in the following form (Galli 2013):

$$\frac{Y_{SZ} D_A^2}{Y_X} \propto C_{X SZ} \frac{\int n_e(r) T(r) dV}{T(R) \int n_e(r) dV}, \quad (24)$$

where

$$C_{X SZ} = \frac{\sigma_T}{m_e c^2} \frac{1}{\mu_e m_p} \approx 1.416 \times 10^{-19} \left(\frac{Mpc^2}{M_\odot keV} \right). \quad (25)$$

The numerator and denominator in Eq.(24) are both approximations of the thermal energy of the cluster. As discussed in Colaço et al. (2019), this ratio would be exactly constant with redshift if no new physics is assumed. As done by

Galli (2013); Colaço et al. (2019); Bora & Desai (2021a), and considering Eq.(11), we can rewrite the ratio in Eq.(23) into

$$\frac{Y_{SZ}D_A^2}{Y_X C_{X SZ}} = C B_F(\phi)^{-3} = C(1 - \zeta(\phi - \phi_0))^{-3}, \quad (26)$$

where C is a constant to be determined. The case of $C \simeq 1$ indicates that the galaxy clusters used in this analysis are isothermal.

We are interested in a possible α variation as predicted by the quintessence model. The quintessence scalar field ϕ evolves via Eqs.(5) and (6), then the constants C and ζ can be determined by observational measurements. As shown in Eq.(12), if the resulting ζ departs from zero significantly, a time variation for α should be established.

4. GALAXY CLUSTER SAMPLES

Large solid angle surveys employing the SZ effect have been carried out with the South Pole Telescope (SPT, Carlstrom et al. (2011)), Planck (P. A. R. Ade, N. Aghanim et al. (Planck Collaboration) 2011a), and the Atacama Cosmology Telescope (ACT, Fowler et al. (2007)). One data set used here is the SZ and X-ray data extracted from Table 1 of P. A. R. Ade, N. Aghanim et al. (Planck Collaboration) (2011a). The SZ effect measurements in the direction of 62 nearby galaxy clusters ($z < 0.5$), which is a sub-sample of the Planck Early Sunyaev-Zel'dovich (ESZ) cluster sample (P. A. R. Ade, N. Aghanim et al. (Planck Collaboration) 2011b), were detected at high signal-to-noise ($S/N \geq 6$) in the first Planck all-sky data set. These galaxy clusters are not contaminated by flares and their morphologies are regular enough that the spherical symmetry can be assumed. They had also been observed by the XMM-Newton telescope, and their Y_X measurements were obtained with the deep XMM-Newton X-ray data (Piffaretti et al. 2011). As done by Galli (2013), cluster A2034 is excluded from the analysis since its redshift estimate is discordant in P. A. R. Ade, N. Aghanim et al. (Planck Collaboration) (2011a); Mantz et al. (2010). So we use 61 Planck-ESZ clusters in this analysis covering the redshift range $0.044 < z < 0.44$. The Y_{SZ} and Y_X parameters are labeled as $D_A^2 Y_{500}$ and $Y_{X,500}$ respectively. Here 500 indicates a radius R_{500} at which the mean matter density of the cluster is 500 times than the critical density of the Universe at the redshift of the cluster. The computation of the Y_{SZ} parameter requires shaping the thermal pressure (P) of the intracluster medium for each galaxy cluster by using the Universal Pressure Profile (Arnaud et al. 2010). Furthermore, the X-ray temperatures are defined within a cylindrical annulus of radius $[0.15 - 0.75]R_{500}$. See Galli (2013); Colaço et al. (2019) for more comments on the data set.

Another data set used in our analysis is the SPT galaxy cluster sample. SPT is a 10m telescope at the South Pole that images the sky at three different frequencies, i.e. 95 GHz, 150 GHz, and 220 GHz (Carlstrom et al. 2011). SPT has detected 516 galaxy clusters via the SZ effect in the 2500 square degree SPT-SZ Survey at $0 < z < 1.8$ with masses $M_{500} \geq 3 \times 10^{14} M_\odot$, and approximately 20 percent of the sample lies at $z > 0.8$ (Bleem et al. 2015). The redshifts of the SPT cluster candidates have been obtained through dedicated optical surveys and follow-up programs (Desai et al. 2012; Song et al. 2012; Saro et al. 2015). Their properties were described in Bleem et al. (2015), among which the redshift values were updated in Bocquet et al. (2019). The Y_{SZ} value of each SPT cluster is measured through integrating the thermal SZ signal in a cylindrical volume within a $0.75'$ -radius aperture. Note their X-ray counterpart, Y_X , is measured within a 3D sphere of radius R_{500} . In order to compare Y_{SZ} with Y_X , one needs to convert the SPT Y_{SZ} values to spherically integrated Y_{SZ} within the same radius at which Y_X was measured. This conversion is performed based on the following expressions (Arnaud et al. 2010):

$$Y_{\text{cyl}}(R_1) = Y_{\text{sph}}(R_b) - \frac{\sigma_T}{m_e c^2} \int_{R_1}^{R_b} 4\pi P(r) \sqrt{r^2 - R_1^2} r dr \quad (27)$$

$$Y_{\text{sph}}(R_2) = \frac{\sigma_T}{m_e c^2} \int_0^{R_2} 4\pi P(r) r^2 dr. \quad (28)$$

Here, $Y_{\text{cyl}}(R_1)$ is the Y_{SZ} parameter measured within a cylindrical aperture of radius R_1 , and $Y_{\text{sph}}(R_2)$ is the Y_{SZ} parameter integrated within a spherical volume of radius R_2 . R_b is the radial extent of the cluster, and $P(r)$ is the gas pressure in the intra-cluster medium. An analytical form of $P(r)$ is needed to calculate the integrations in Eqs.(27-28), for which we adopt the Universal Pressure Profile suggested by Arnaud et al. (2010). Following Bora & Desai (2021a), we set $R_b = 10R_{500}$. Since the SPT observation gave Y_{SZ} values in terms of an aperture of $0.75'$, $R_1 = 0.75'D_A$ is required in Eq.(27). We put $R_2 = R_{500}$ in Eq.(28), concordant with the radius at which the SPT Y_X is measured. In order to be less dependent on the free parameters involved in the Universal Pressure Profile of $P(r)$ and make the

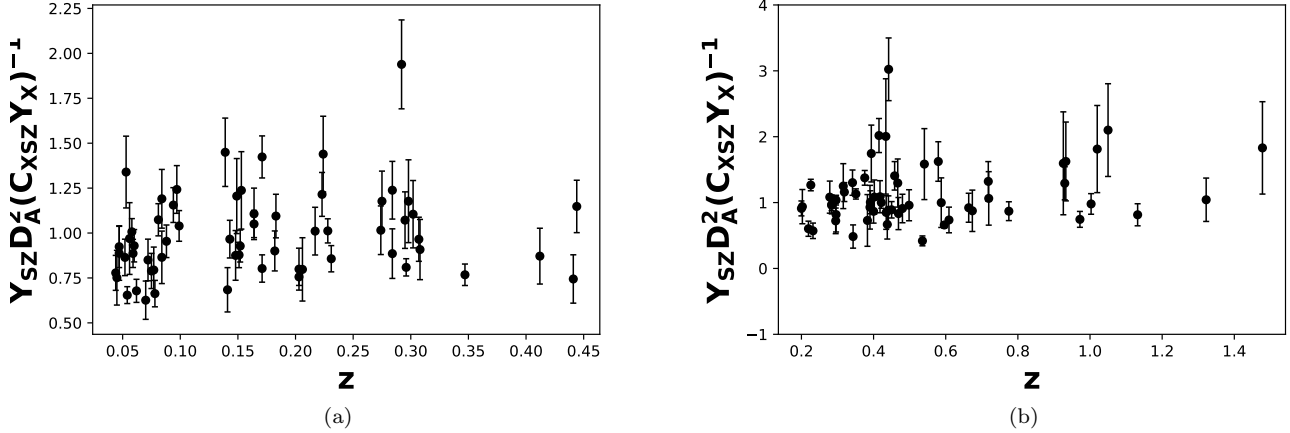


Figure 1. The observed ratio $Y_{SZ}D_A^2/Y_X C_{XSZ}$. They are calculated from (a) the Planck galaxy cluster sample, (b) the SPT galaxy cluster sample.

computation more reliable, instead of calculating $Y_{\text{sph}}(R_{500})$ directly by Eq.(28), we estimate $Y_{\text{sph}}(R_{500})$ via calculating the ratio of $Y_{\text{sph}}(R_{500})$ to $Y_{\text{cyl}}(0.75'D_A)$ from Eqs.(27) and (28).

The XMM-Newton X-ray observations of 73 of these SZE-selected clusters have been performed by SPT collaboration members or various non-SPT small programs, among which 15 clusters were excluded due to their low data quality or low redshift ($z < 0.2$). Thus, a sample of 58 clusters with redshift range $0.2 < z < 1.5$ is used for analysis. The sample has a median mass and redshift of $M_{500} = 4.77 \times 10^{14} M_{\odot}$ and $z_{\text{med}} = 0.45$ respectively, and five clusters lie at $z > 1$. The X-ray observable-mass scaling relations of these clusters were studied in Bulbul et al. (2019), and the details of their XMM-Newton observations, especially Y_X values, can be found in Table 1 of Bulbul et al. (2019). Same as the Planck counterparts, the X-ray observables of the sample were measured at R_{500} .

5. ANALYSIS AND RESULTS

In order to constrain the parameters of Eq. 26, we minimize the following negative log-likelihood function:

$$-2 \ln L = \sum_{i=1}^N \ln 2\pi\sigma_i^2 + \sum_{i=1}^N \frac{[R_{\text{obs},i} - C(1 - \zeta(\phi - \phi_0))^{-3}]^2}{\sigma_i^2}, \quad (29)$$

where

$$R_{\text{obs},i} = \frac{(Y_{SZ}D_A^2)_i}{Y_{X,i}C_{XSZ}}. \quad (30)$$

denotes the observed values of the ratio in Eq.(26) for galaxy clusters, N is the total number of clusters, and σ_i is the total uncertainty inherited from the observations $(Y_{SZ}D_A^2)_i$ and $Y_{X,i}$, plus an intrinsic scatter term σ_{int} , that is

$$\sigma_i^2 = \left(\frac{\sigma_{SZ,i}}{Y_{X,i}C_{XSZ}} \right)^2 + \left(\frac{(Y_{SZ}D_A^2)_i \sigma_{X,i}}{Y_{X,i}C_{XSZ}} \right)^2 + \sigma_{\text{int}}^2. \quad (31)$$

where $\sigma_{SZ,i}$ and $\sigma_{X,i}$ denote the uncertainty of $(Y_{SZ}D_A^2)_i$ and $Y_{X,i}$, respectively. The advantage of using log-likelihood against the commonly used χ^2 criterion is that the log-likelihood function can accommodate the optimization of the intrinsic uncertainty. Thus, for the SPT sample the parameter space to be optimized is $\{C, \zeta, \sigma_{\text{int}}\}$. For the Planck sample, we followed Galli (2013) and set $\sigma_{\text{int}} = 0.17$. So the parameter space of the Planck sample is reduced to $\{C, \zeta\}$, and the objective function (29) becomes equivalent to the χ^2 criterion. Our experiment shows different cosmological parameters only have marginal effect on the result, so we fix the cosmological parameters as $H_0 = 67.4$, $\Omega_m = 0.315$ in the implementation of quintessence model.

Unlike the Planck cluster sample for which the product of Y_{SZ} and D_A^2 i.e. $Y_{SZ}D_A^2$, is already given as an observational quantity, for SPT data we need to estimate the angular diameter distance to each galaxy cluster via,

$$D_A = \frac{1}{1+z} \int_0^z \frac{cdz'}{H(z')}, \quad (32)$$

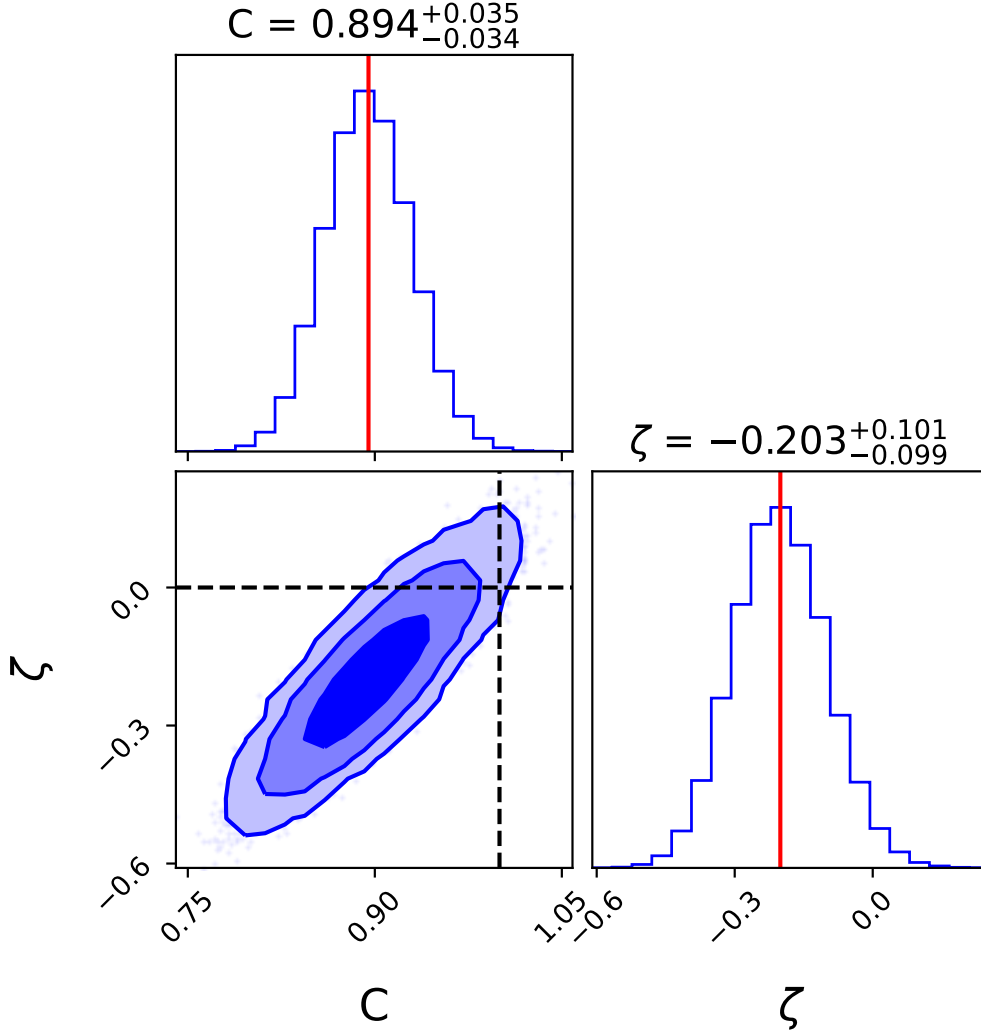


Figure 2. Contours of 1σ , 2σ and 3σ on the $\zeta - C$ plane and the corresponding 1-D marginalized likelihood distributions for the Planck clusters.

while $H(z)$ is calculated by the quintessence model (i.e. Eqs.(5) and (6)).

We maximize the likelihood using the emcee MCMC sampler (Foreman-Mackey et al. 2013). The results on the Planck cluster sample and those on the SPT cluster sample are given in Fig.2 and Fig.3, respectively, which display the 68%, 95%, and 99% confidence level plots along with the marginalized one-dimensional distribution of each parameter. We obtain $\zeta = -0.203^{+0.101}_{-0.099}$, $C = 0.894^{+0.035}_{-0.034}$ from the Planck sample and $\zeta = -0.043^{+0.165}_{-0.148}$, $C = 0.972^{+0.136}_{-0.118}$, $\sigma_{int} = 0.259^{+0.047}_{-0.040}$ from the SPT sample. We find from Fig.2 that the point ($\zeta = 0, C = 1$) is located within the 3σ contour for the Planck sample. Therefore, our results indicate that there is no significant evidence for nonzero ζ , implying no time variation in α . Furthermore, since $C = 1$ holds within 3σ and 1σ for the Planck sample and the SPT sample respectively, we conclude that the isothermality assumption of the temperature profile is applicable quite well for both the Planck cluster sample and the SPT cluster sample. It seems that the intrinsic uncertainty of the SPT data ($\sigma_{int} = 0.259$) is heavier than that of the Planck data ($\sigma_{int} = 0.17$). Considering they stem from different analysis method, this conclusion needs further validation.

6. CONCLUSIONS

We explore the possible time variation of the fine structure constant α based on the scaling relation $Y_{SZ}D_A^2/C_{XYZ}Y_X$ calculated from galaxy cluster measurements. Following Colaço et al. (2019), this ratio depends on the fine structure

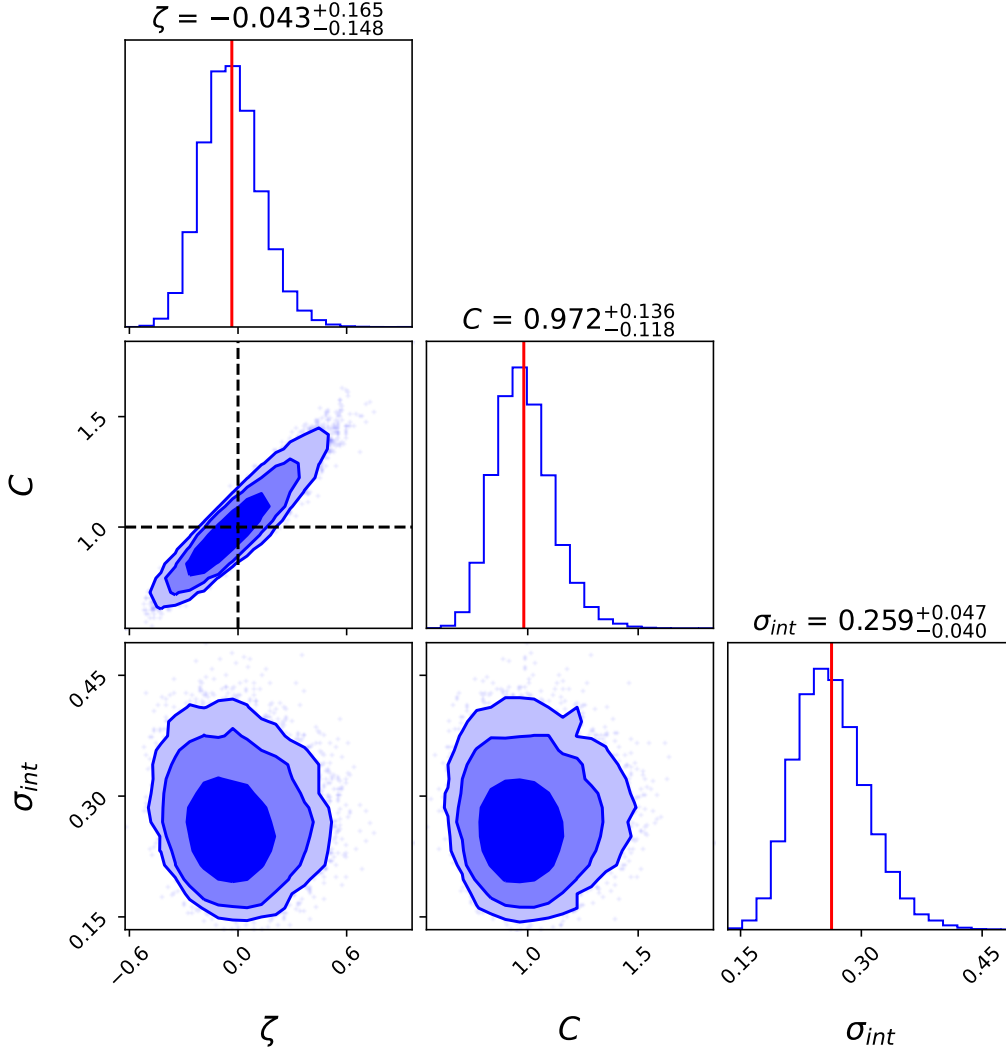


Figure 3. Contours of 1σ , 2σ and 3σ on the 2-D parameter planes and the corresponding 1-D marginalized likelihood distributions for the SPT clusters. The red line represents the mean value of each parameter. The dashed lines in the $\zeta - C$ plane mark $\zeta = 0$ and $C = 1$, which represents $\alpha = \alpha_0$ and the isothermality assumption, respectively.

constant through the Thompson cross-section and is also affected by the violation of cosmic distance duality relation through the cluster gas mass. Instead of the frequently used runaway dilaton models, we use the quintessence model to provide the theoretical mechanism of generating time-varying α . Different from the runaway dilaton model, for which the redshift dependence of the dilaton field is explicitly approximated by $\phi(z) = 1 - \gamma \ln(1+z)$ at low and intermediate redshifts, the dynamics of the quintessence scalar field is given by an evolution procedure described using Eqs.(5) and (6). The resulting equality $Y_{SZ} D_A^2 / Y_X C_{XSZ} = C(1 - \zeta(\phi - \phi_0))^{-3}$ is derived to link the quintessence field with the cluster observations.

We use the data of two cluster samples to constrain the variation of the fine structure constant. One sample is the observations of 61 galaxy clusters reported by the Planck collaboration, and another is the 58 galaxy clusters selected by the SPT-SZ observation. The X-ray counterpart (i.e. Y_X) of both the samples has been observed by the XMM-Newton observations. We give different treatments to the intrinsic uncertainty from the two data sets. For the Planck sample, we set $\sigma_{int} = 0.17$ directly, while for the SPT sample σ_{int} is taken as a free parameter and the determination of its best value is fused in the optimization procedure. In this way, the intrinsic uncertainty σ_{int} for the SPT sample depends on the dispersion of angular diameter distance D_A and thus is affected by the uncertainties of the cosmological parameters (i.e., H_0 and Ω_m) indirectly. Our analyses show no significant evidence for the fine

structure constant α varying with redshift, consistent with previous galaxy cluster-based results (Galli 2013; Colaço et al. 2019; Bora & Desai 2021a,b). The constant C was found to approach unity sufficiently, indicating the isothermal temperature profile is universal for describing the galaxy clusters.

The number of galaxy clusters available is mainly limited by the current X-ray observations. For example, among the 516 clusters detected by the SPT-SZ survey, only 73 clusters have corresponding XMM-Newton X-ray observations. The eROSITA satellite, which has been launched in 2019, will perform the first imaging all-sky survey in the medium energy X-ray range and detect 50-100 thousand galaxy clusters (Hofmann et al. 2017). More detailed and richer observations in future may let us check whether the conclusion drawn in this paper is still valid in different redshift domains or not. We expect the problem of α variation would get a better answer with enlarging galaxy cluster samples.

1 We thank the anonymous referee for helpful and constructive feedback. This work was supported by the National Key
 2 R&D Program of China (2017YFA0402600), the Natural Science Foundation of Shandong Province, China (Grant
 3 NO.ZR2019MA059), and the National Natural Science Foundation of China (grant No.11929301). ZZ is supported
 4 in part by NASA grant 15-WFIRST15-0008, Cosmology with the High Latitude Survey Roman Science Investigation
 5 Team (SIT). KB acknowledges Department of Science and Technology, Government of India for providing the financial
 6 support under DST-INSPIRE Fellowship program.

APPENDIX

To demonstrate that the constraints on the time variation of α is insensitive to the cosmological parameters, we repeat the analysis for both data-sets treating H_0 and Ω_m as free parameters. We assume Gaussian bivariate prior distributions on H_0 and Ω_m with the following expression

$$p^{priors}(x) = \frac{1}{2\pi\sqrt{|\Sigma|}} \exp\left(-\frac{1}{2}(x-d)\Sigma^{-1}(x-d)\right), \quad (1)$$

where $x = \{H_0, \Omega_m\}$, and their mean values $d = \{67.36, 0.3153\}$ and covariance matrix $\Sigma = \begin{pmatrix} 0.287 & -3.89 \times 10^{-3} \\ -3.89 \times 10^{-3} & 5.37 \times 10^{-5} \end{pmatrix}$ are derived from the CosmoMC chains of Planck 2018

TT,TE,EE+lowE+lensing (Chen et al. 2019). We get $C = 0.894^{+0.036}_{-0.034}$, $\zeta = -0.202^{+0.103}_{-0.101}$ for the Planck clusters (see Fig.4) and $\zeta = -0.045^{+0.166}_{-0.145}$, $C = 0.971^{+0.136}_{-0.117}$, $\sigma_{int} = 0.259^{+0.047}_{-0.039}$ for the SPT clusters (see Fig.5). One can see that compared to the results obtained with fixed H_0 and Ω_m , the difference between the both analyses is insignificant.

REFERENCES

- Arnaud, M., Pratt, G., Piffaretti, R., et al. 2010, *Astron. Astrophys.*, 517, A92
- Barrow, J. D. 1987, *Phys. Rev. D*, 35, 1805
- Barrow, J. D., & Graham, A. A. H. 2013, *Phys. Rev. D*, 88, 103513
- Barrow, J. D., & Li, B. 2008, *Phys. Rev. D*, 78, 083536
- Barrow, J. D., & Lip, S. Z. W. 2012, *Phys. Rev. D*, 85, 023514
- Barrow, J. D., Magueijo, J., & Sandvik, H. B. 2002a, *Phys. Rev. D*, 66, 043515
- Barrow, J. D., & Mota, D. F. 2003, *Class. Quantum Grav.*, 20, 2045
- Barrow, J. D., Sandvik, H. B., & Magueijo, J. 2002b, *Phys. Rev. D*, 65, 063504
- Barrow, J. D., & Tipler, F. J. 1986, *The Anthropic Cosmological Principle* (Oxford: Oxford University Press)
- Bekenstein, J. D. 1982, *Phys. Rev. D*, 25, 1527
- Berengut, J. C., Flambaum, V. V., Ong, A., et al. 2013, *Phys. Rev. Lett.*, 111, 010801
- Bleem, L. E., Stalder, B., de Haan, T., & et al. 2015, *Astrophys. J. Suppl. Ser.*, 216, 27
- Bocquet, S., Dietrich, J. P., Schrabback, T., & et al. 2019, *Astrophys. J.*, 878, 55
- Bora, K., & Desai, S. 2021a, *Journal of Cosmology and Astroparticle Physics*, 02, 012
- . 2021b, arXiv:2104.00974v1
- Bulbul, E., Chiu, I. N., Mohr, J. J., & et al. 2019, *Astrophys. J.*, 871, 50

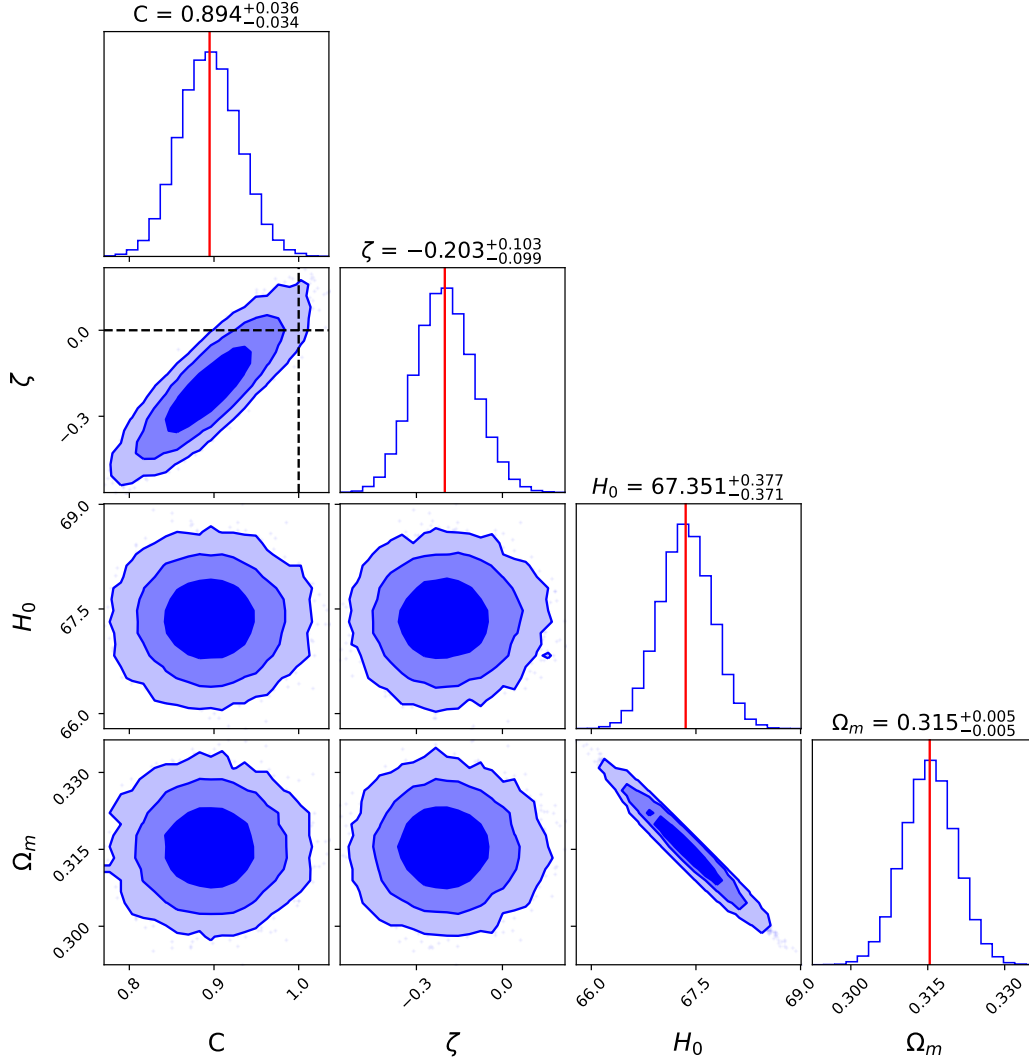


Figure 4. Contours of 1σ , 2σ and 3σ on the 2-parameter planes and the corresponding 1-D marginalized likelihood distributions for the Planck clusters.

Carlstrom, J. E., Ade, P. A. R., Aird, K. A., & et al. 2011, Publications of the Astronomical Society of the Pacific, 123, 568

Chand, H., Srianand, R., Petitjean, P., & Aracil, B. 2004, A&A, 417, 853

Chen, G., & Ratra, B. 2011, Publications of the Astronomical Society of the Pacific, 123, 1127

Chen, L., Huang, Q.-G., & Wang, K. 2019, Journal of Cosmology and Astroparticle Physics, 02, 028

Chodos, A., & Detweiler, S. 1980, Phys. Rev. D, 21, 2167

Clara, M. T., & Martins, C. J. A. P. 2020, A&A, 633, L11

Colaço, L. R., Gonzalez, J. E., & Holanda, R. F. L. 2020a, arXiv eprints arXiv:2010.04021

Colaço, L. R., Holanda, R. F. L., & Silva, R. 2020b, arXiv eprints arXiv: 2004.08484

Colaço, L. R., Holanda, R. F. L., Silva, R., & Alcaniz, J. S. 2019, Journal of Cosmology and Astroparticle Physics, 03, 014

Copeland, E. J., Nunes, N. J., & Pospelov, M. 2004, Phys. Rev. D, 69, 023501

Damour, T., & Dyson, F. 1996, Nucl. Phys. B, 480, 37

Desai, S., Armstrong, R., Mohr, J. J., et al. 2012, Astrophys. J., 757, 83

Dirac, P. 1937, Nature, 139, 323

Dodson, S., & Schmidt, F. 2020, Modern Cosmology, 2nd edn. (Amsterdam, Boston: Academic Press)

Farajollahi, H., & Salehi, A. 2012, Journal of Cosmology and Astroparticle Physics, 2012, 041

Foreman-Mackey, D., Hogg, D. W., Lang, D., & Goodman, J. 2013, Publ. Astron. Soc. Pac., 125, 306

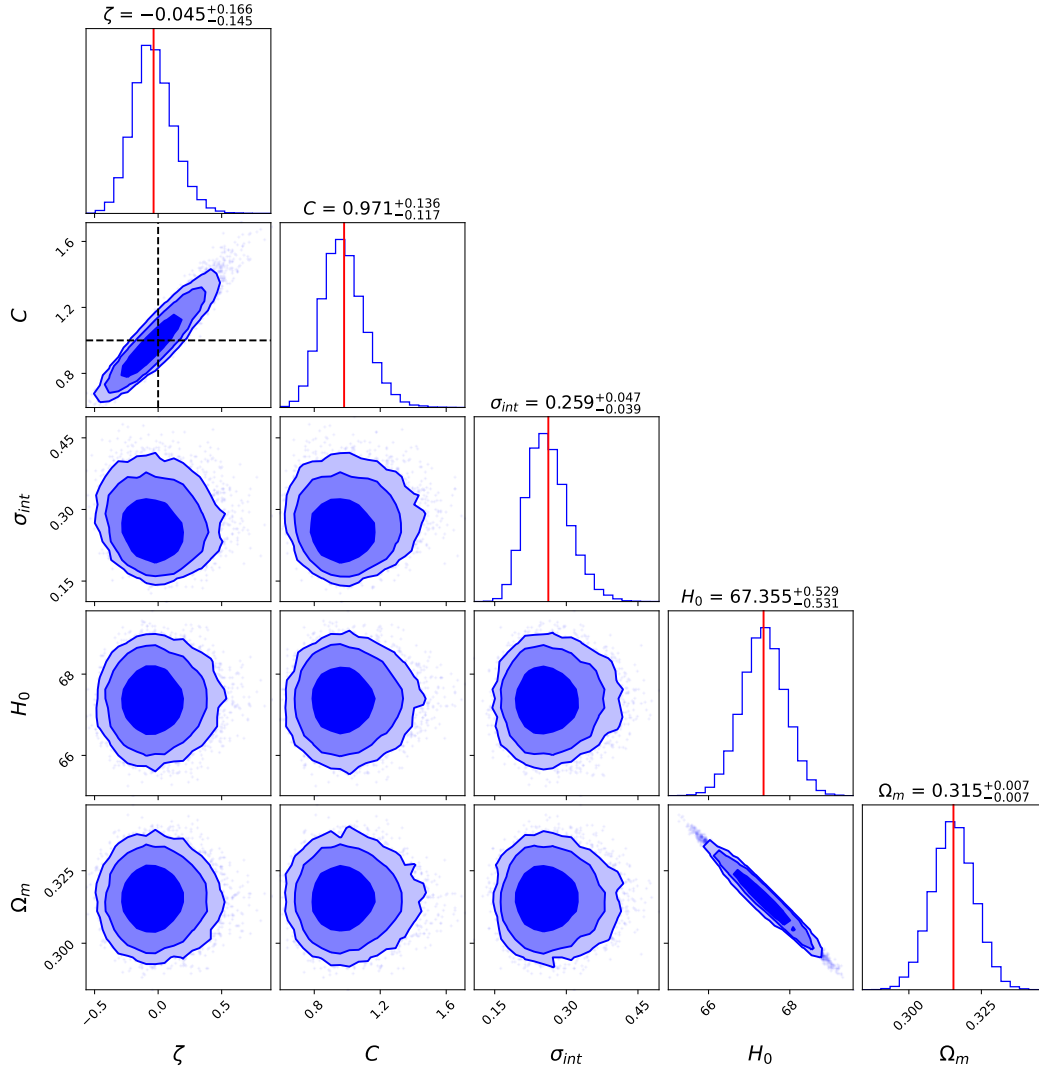


Figure 5. Contours of 1σ , 2σ and 3σ on the 2-parameter planes and the corresponding 1-D marginalized likelihood distributions for the SPT clusters.

Fowler, J. W., Niemack, M. D., Dicker, S. R., & et al. 2007, *Applied Optics*, 46, 3444
 Galli, S. 2013, *Phys. Rev. D* 87 (2013), 87, 123516
 Gamow, G. 1967, *Phys. Rev. Lett.*, 19, 759
 Goncalves, R. S., Holanda, R. F. L., & Alcaniz, J. S. 2012, *Mon. Not. Roy. Astron. Soc.*, 420, L43
 Hart, L., & Chluba, J. 2018, *MNRAS*, 474, 1850
 Hees, A., Minazzoli, O., & Larena, J. 2014, *Phys. Rev. D*, 90, 124064
 Hees, A., Do, T., Roberts, B. M., et al. 2020, *Phys. Rev. Lett.*, 124, 081101
 Hofmann, F., Sanders, J. S., Clerc, N., et al. 2017, *Astron. & Astrophys.*, 606, A118,
 doi: [10.1051/0004-6361/201730742](https://doi.org/10.1051/0004-6361/201730742)
 Holanda, R. F. L., Busti, V. C., L. R. Colaço, J. S. A., & Landau, S. J. 2016a, *JCAP*, 08, 055

Holanda, R. F. L., Colaço, L. R., Gonçalves, R. S., & Alcaniz, J. S. 2017, *Physics Letters B*, 767, 188
 Holanda, R. F. L., Landau, S. J., Alcaniz, J. S., Sánchez G., I. E., & Busti, V. C. 2016b, *JCAP*, 2016, 047
 Iocco, F., Mangano, G., Miele, G., Pisanti, O., & Serpico, P. D. 2009, *Phys. Rep.*, 472, 1
 King, J. A., Webb, J. K., Murphy, M. T., et al. 2012, *MNRAS*, 422, 3370
 Kolb, E. W., Perry, M. J., & Walker, T. P. 1986, *Phys. Rev. D*, 33, 869
 Kravtsov, A. V., Vikhlinin, A., & Nagai, D. 2006, *Astrophys. J.*, 650, 128
 Lamoreaux, S. K., & Torgerson, J. R. 2004, *Phys. Rev. D*, 69, 12170

- Mantz, A., Allen, S. W., Ebeling, H., Rapetti, D., & Drlica-Wagner, A. 2010, *Mon. Not. R. Astron. Soc.*, 406, 1773
- Marciano, W. J. 1984, *Phys. Rev. Lett.*, 52, 489
- Marra, V., & Rosati, F. 2005, *J. Cosmol. Astropart. Phys.*, 5, 011
- Martins, C. J. A. P. 2017, *Rep. Prog. Phys.*, 80, 126902
- Morel, L., Yao, Z., Cladé, P., & Guellati-Khélifa, S. 2020, *Nature*, 588, 61
- Mosquera, M. E., & Civitaresse, O. 2013, *A&A*, 551, A122
- Murphy, M., Webb, J., Flambaum, V., et al. 2001a, *MNRAS*, 327, 1244
- . 2001b, *MNRAS*, 327, 1208
- Murphy, M., Webb, J., Flambaum, V., Prochaska, J., & Wolfe, A. 2001c, *MNRAS*, 327, 1237
- Murphy, M. T., Flambaum, V. V., Webb, J. K., et al. 2004, in *Lecture Notes in Physics*, Vol. 648, *Astrophysics, Clocks and Fundamental Constants*, ed. S. G. Karshenboim & E. Peik (Berlin: Springer Verlag), 131–150
- Murphy, M. T., Webb, J. K., & Flambaum, V. V. 2003, *MNRAS*, 345, 609
- . 2007, *Physical Review Letters*, 99, 239001
- . 2008, *MNRAS*, 384, 1053
- O’Bryan, J., Smidt, J., Bernardis, F. D., & Cooray, A. 2015, *ApJ*, 798, 18
- P. A. R. Ade, N. Aghanim et al. (Planck Collaboration). 2011a, *Astron. Astrophys.*, 536, A11
- . 2011b, *Astron. Astrophys.*, 536, A8
- Padmanabhan, T. 2003, *Phys. Rep.*, 380, 235
- Park, C.-G., & Ratra, B. 2019, *Astrophysics and Space Science*, 364, 134
- Peebles, P. J. E., & Ratra, B. 1988, *ApJ*, 325, L17, 325, L17
- Piffaretti, R., Arnaud, M., Pratt, G., Pointecouteau, E., & Melin, J.-B. 2011, *Astron. Astrophys.*, 534, A109
- PLANCK Collaboration. 2015, *A&A*, 580, A22
- Planck Collaboration. 2020, *A&A*, 641, A6
- Samushia, L., & Ratra, B. 2006, *The Astrophysical Journal*, 650, L5, doi: [10.1086/508662](https://doi.org/10.1086/508662)
- . 2009, *The Astrophysical Journal*, 701, 1373, doi: [10.1088/0004-637x/701/2/1373](https://doi.org/10.1088/0004-637x/701/2/1373)
- Sandvik, H. B., Barrow, J. D., & Magueijo, J. 2002, *Phys. Rev. Lett.*, 88, 031302
- Saro, A., Bocquet, S., Rozo, E., et al. 2015, *Monthly Notices of the Royal Astronomical Society*, 454, 2305, doi: [10.1093/mnras/stv2141](https://doi.org/10.1093/mnras/stv2141)
- Song, J., Zenteno, A., Stalder, B., et al. 2012, *The Astrophysical Journal*, 761, 22, doi: [10.1088/0004-637x/761/1/22](https://doi.org/10.1088/0004-637x/761/1/22)
- Srianand, R., Chand, H., Petitjean, P., & Aracil, B. 2004, *Phys. Rev. Lett.*, 92, 121302
- Sunyaev, R. A., & Zel’dovich, Y. B. 1972, *Comments on Astrophysics & Space Physics*, 4, 173
- Teller, E. 1948, *Phys. Rev.*, 73, 801
- Uzan, J.-P. 2003, *Rev. Mod. Phys.*, 75, 403
- . 2011, *Living Rev. Rel.*, 14, 2
- Wang, K., & Chen, L. 2020, *Eur. Phys. J. C*, 80, 570
- Webb, J. K., Flambaum, V. V., Churchill, C. W., Drinkwater, M. J., & Barrow, J. D. 1999, *Phys. Rev. Lett.*, 82, 884
- Webb, J. K., King, J. A., Murphy, M. T., et al. 2011, *Phys. Rev. Lett.*, 107, 191101
- Webb, J. K., Murphy, M. T., Flambaum, V. V., et al. 2001, *Phys. Rev. Lett.*, 87, 091301